

Supporting Information

Table S1. Binding constant (K_b) and thermodynamic parameters for interaction of IMQ with RIF at different temperatures.

S.No.	T(K)	$K_b (\times 10^4 \text{ M}^{-1})$	ΔG (kJ mol $^{-1}$)	ΔH (kJ mol $^{-1}$)	ΔS (J mol $^{-1}$ K $^{-1}$)
1	298	7.29	-27.8	-41.77	-46.90
2	303	5.88	-27.56		
3	308	4.34	-27.33		
4	313	3.26	-27.09		

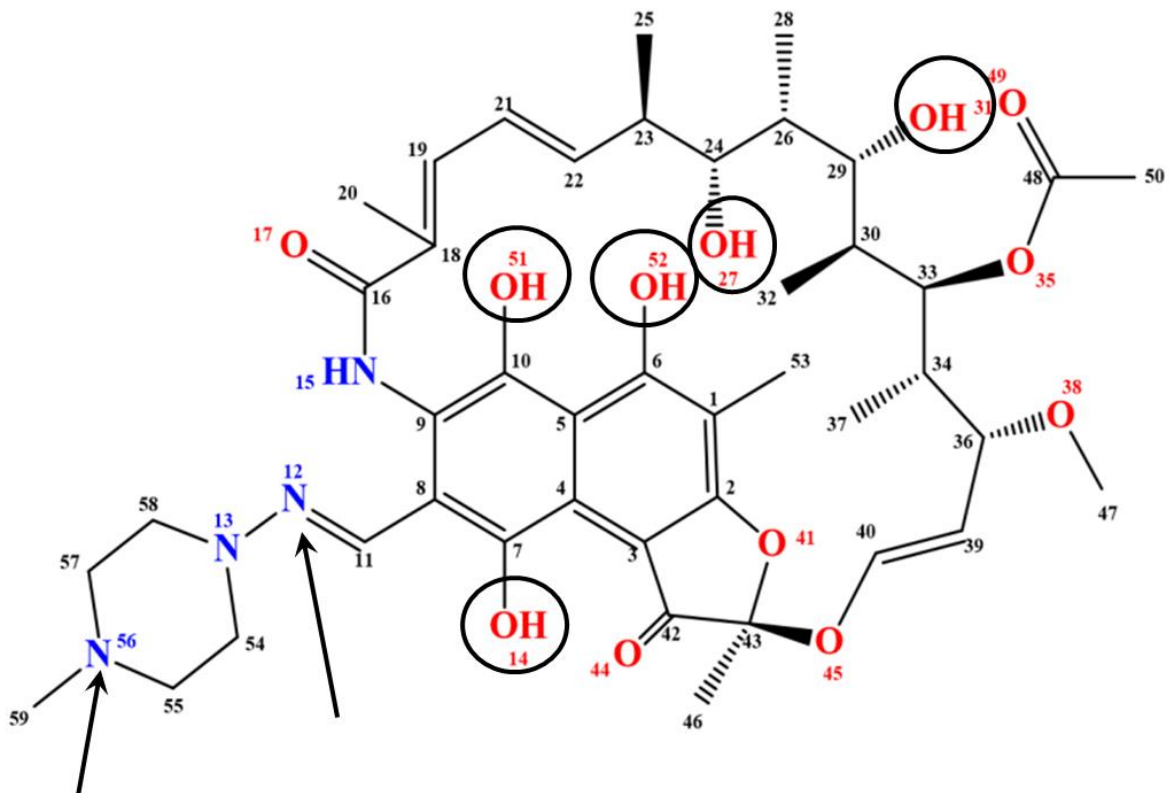
Table S2. Fluorescence decay transients of IMQ on gradual addition of RIF. The excitation wavelength

is $\lambda_{\text{ex}} = 291 \text{ nm}$. $\tau_{\text{av}} = (\tau_1 \times \alpha_1) + (\tau_2 \times \alpha_2) / (\alpha_1 + \alpha_2)$

Sample	λ_{em}	$\tau_1 \text{ (ns)}$	α_1	$\tau_2 \text{ (ns)}$	α_2	$\tau_{\text{av}} \text{ (ns)}$	χ^2
IMQ only	320 nm	1.5	84	3.5	16	1.85	1.5
IMQ + RIF 20 μM		1.6	85	3.7	15	1.89	1.25
IMQ + RIF 39 μM		1.7	85	4	15	2.02	1.49
IMQ only	350 nm	1.5	65	3.9	35	2.3	1.3
IMQ + RIF 20 μM		1.57	66	3.9	34	2.4	1.14
IMQ + RIF 39 μM		1.57	65	3.9	35	2.4	1.26
IMQ only	370 nm	1.5	59	3.9	41	2.5	1.17
IMQ + RIF 20 μM		1.5	57	3.9	43	2.5	1.18
IMQ + RIF 39 μM		1.6	59	4	41	2.55	1.1

Table S3. Optimized energies of Non-ionic and Zwitter ionic forms of RIF. In case of Zwitterionic form, we removed hydrogen from hydroxyl groups and placed at N12 or N56. The highlighted is the most stable among all structural isomers.

Complex	¹ N12 (Without PCM)	² N12 (PCM)	³ N56 (PCM)
RIF _{Non-ionic}	-2795.879834	-2795.925947	-2795.925947
O51	-2795.847019	-2795.897676	-2795.904811
O52(RIF_{Zwitt.})	-2795.898564	-2795.942526	-2795.941415
O14	-2795.871932	-2795.919611	-2795.892875
O27	-2795.870692	-2795.864767	-2795.892873
O31	-2795.870693	-2795.912363	-2795.878313



¹ First column represents energies of zwitter ionic form of RIF deprotonated from encircled oxygens 51, 52, 14, 27, 31 and protonated on nitrogen 12 (-N=NH⁺-) as shown in the figure.

² Second column represents calculations on first column with PCM model.

³ Third column denotes same deprotonation but protonation on nitrogen at 56 position.

Table S4. Estimation of orientation factor (k^2) and energy transfer rates (k_{ET}) from MD simulation.

Complexes	Mean Distance, Å	Estimated Forster radius, R_0 , Å	Orientation factor, k^2	Estimated energy transfer rate, $k_{ET} (\times 10^9 \text{ s}^{-1})$
COM-ZWR:IMQ	9.091	13.99	0.03786`	5.01
RING-ZWR:IMQ	14.44	22.22	0.21474	5.01
ANSA-ZWR:IMQ	12.29367	18.91	0.11732	4.99
COM-NIR:IMQ	6.4417	9.91	0.01846	5
RING-NIR:IMQ	10.3514	15.92	0.10995	4.99
ANSA-NIR:IMQ	9.45353	14.5439	0.057	5

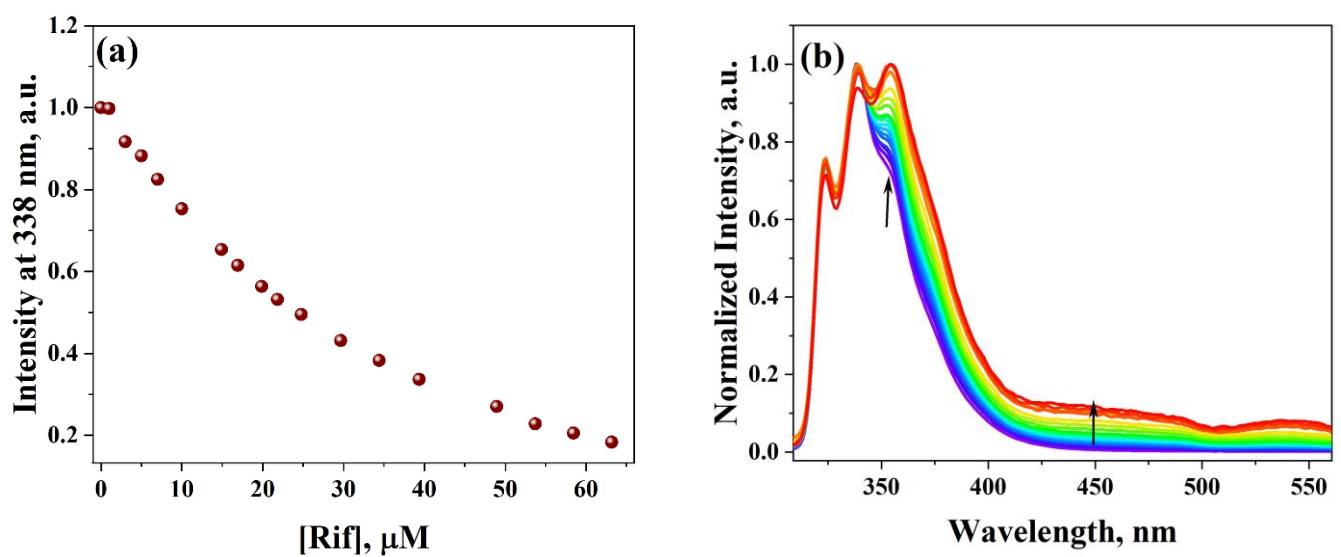


Fig. S1. (a) Relative change in fluorescence intensity of IMQ at 338 nm and (b) normalized emission spectra of IMQ (0.75 μ M) in the presence of RIF (1 μ M to 63 μ M) in PBS (pH = 7.4).

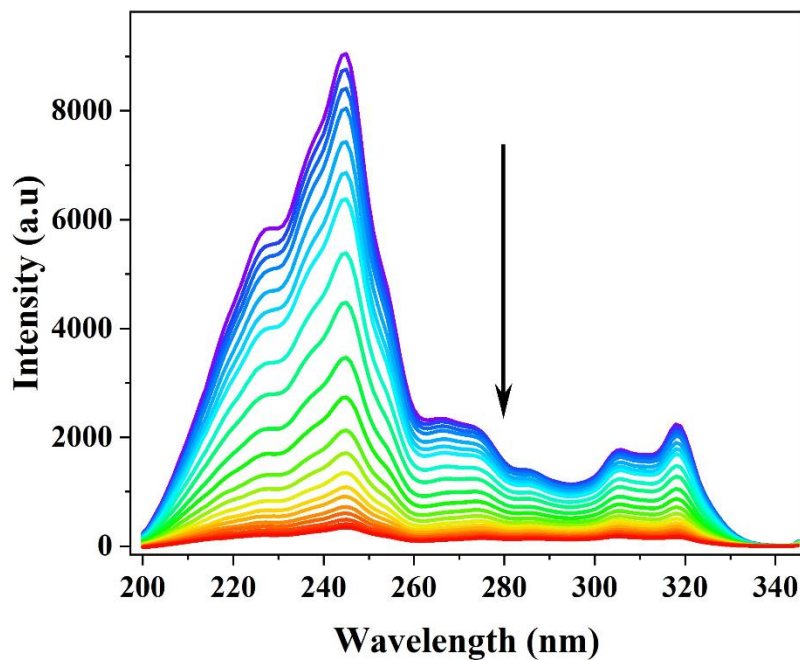


Fig. S2. Steady state excitation spectra of IMQ in the presence of RIF (1.6 μ M to 49.8 μ M) in PBS (pH = 7.4). Emission wavelength is 350 nm. Arrow indicates the direction of increasing concentration of RIF.

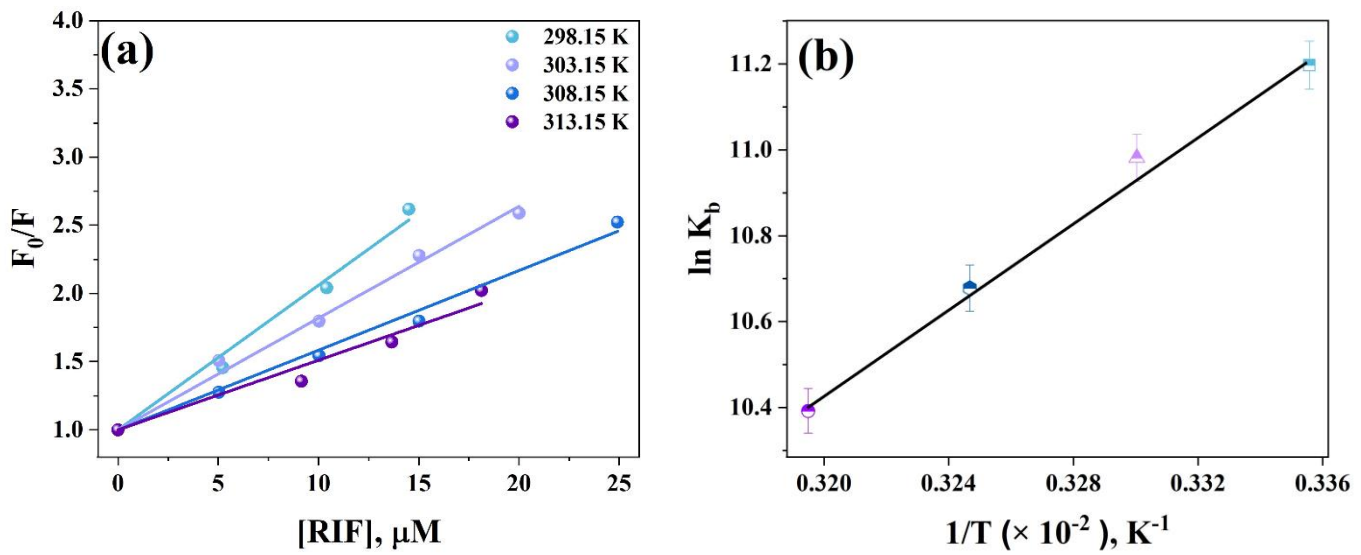


Fig. S3. (a) Stern-Volmer plot and (b) Van't Hoff plot of RIF induced quenching in IMQ at 298, 303, 308 and 313K temperatures and at pH = 7.4.

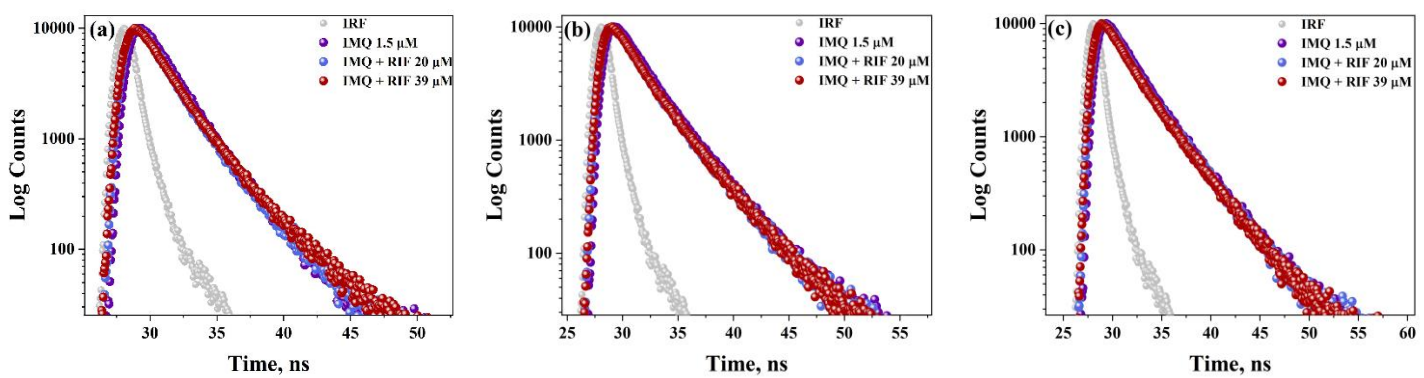


Fig. S4. Fluorescence decay transients of IMQ in absence and presence of RIF at $\lambda_{\text{ex}} = 290 \text{ nm}$ and (a) $\lambda_{\text{em}} = 320 \text{ nm}$ (b) $\lambda_{\text{em}} = 350 \text{ nm}$ (c) $\lambda_{\text{em}} = 370 \text{ nm}$ at pH = 7.4.

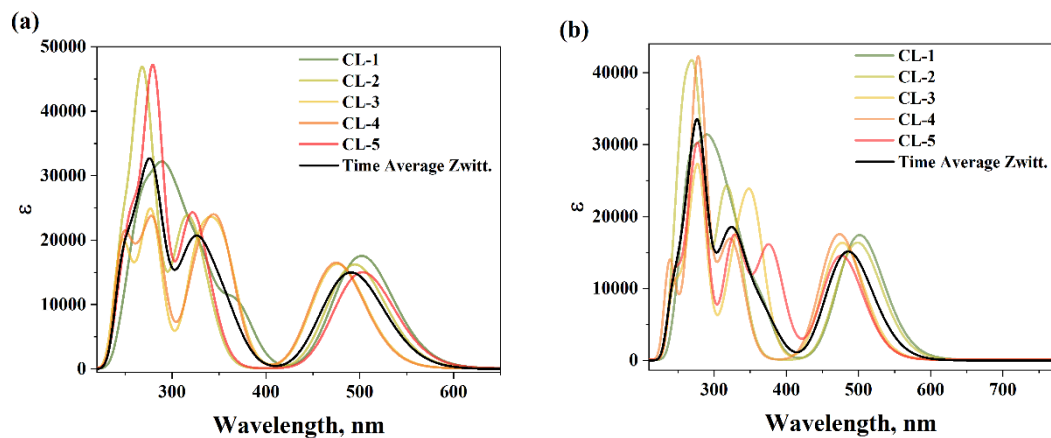


Fig. S5. Absorption spectra computed (CAM-B3LYP functional) from SP (a) and optimized geometries (b) collected from the MD simulation trajectories of RIF_{Zwitt}-IMQ.

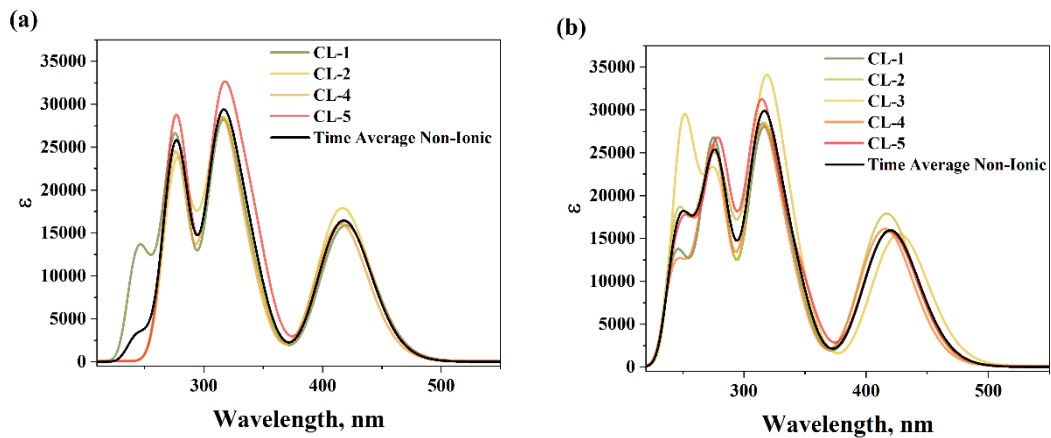


Fig. S6. Absorption spectra computed (CAM-B3LYP functional) from SP (a) and optimized geometries (b) collected from the MD simulation trajectories of RIF_{Non-ionic}-IMQ.

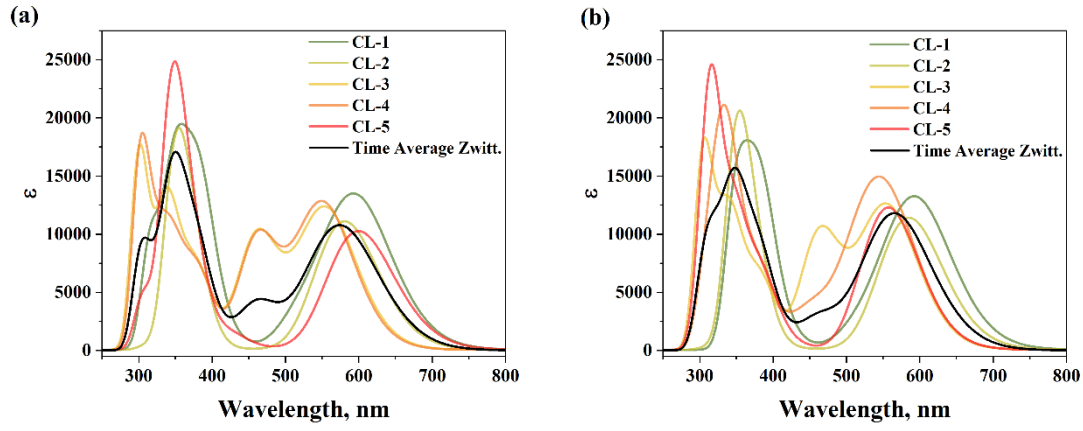


Fig. S7. Absorption spectra computed (B3LYP functional) from SP (a) and optimized geometries (b) collected from the MD simulation trajectories of RIF_{Zwitt.}-IMQ.

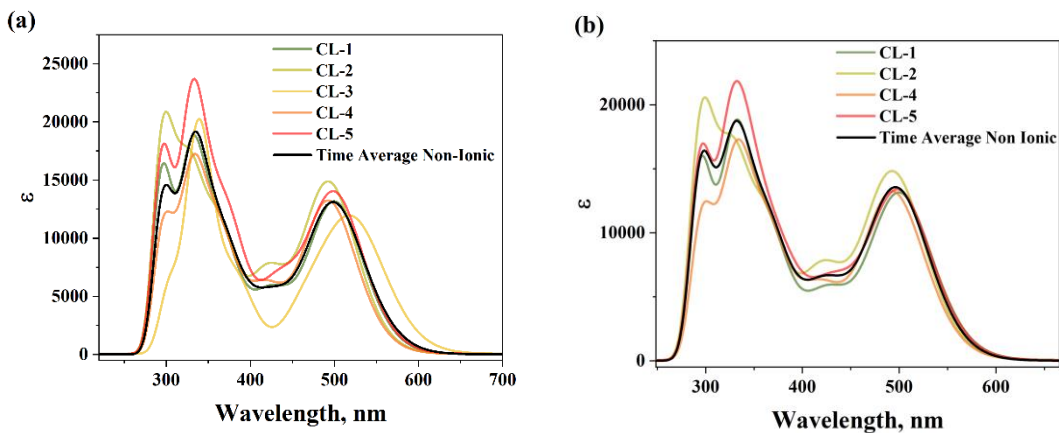


Fig. S8. Absorption spectra computed (B3LYP functional) from SP (a) and optimized geometries (b) collected from the MD simulation trajectories of RIF_{Non-ionic}-IMQ.

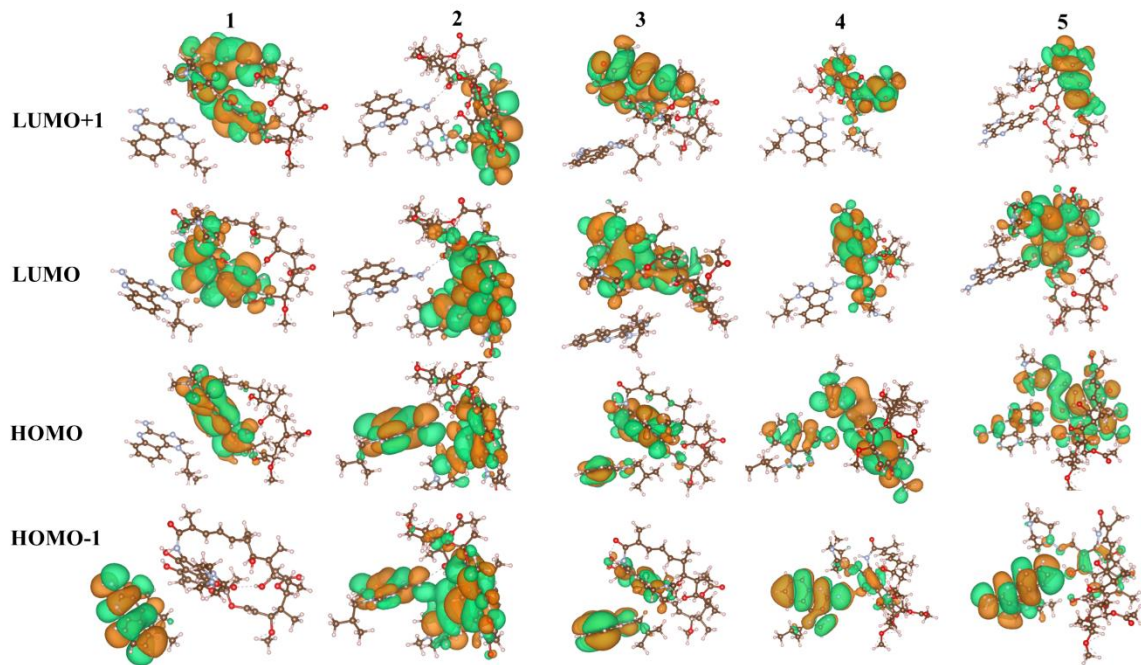


Fig. S9. Molecular Orbital Diagram in MD simulation snapshots for RIF_{Non-ionic}-IMQ complex.

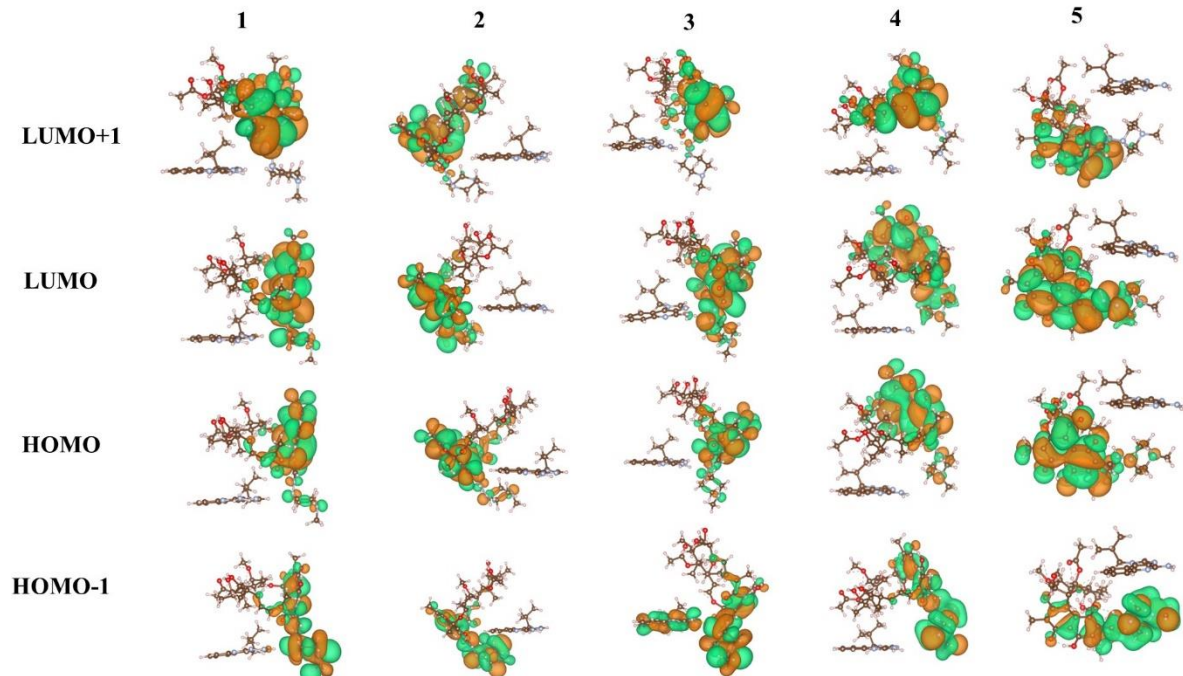


Fig. S10. Molecular Orbital Diagram in MD simulation snapshots for RIF_{Zwitt.}-IMQ complex.

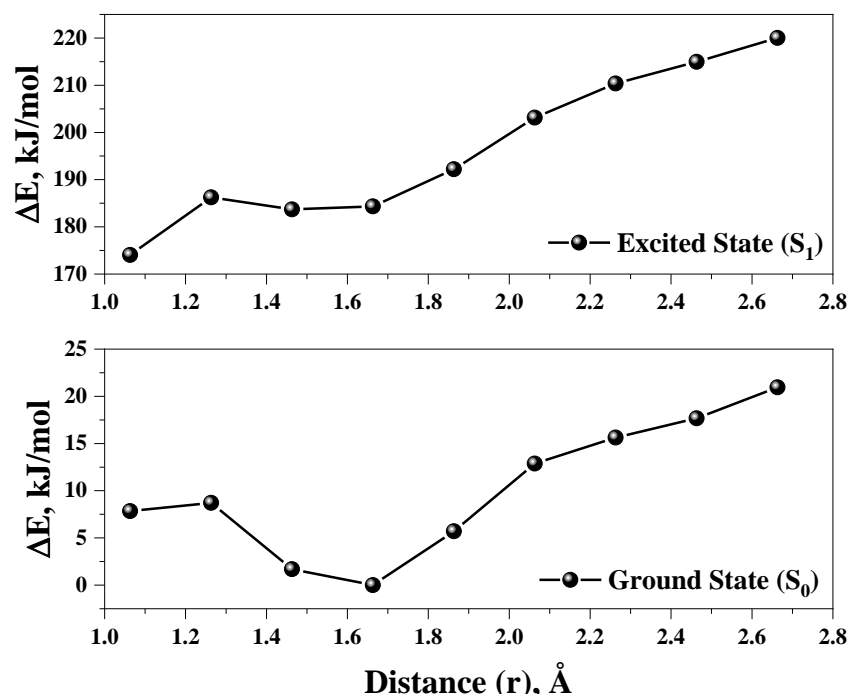


Fig. S12. Potential Energy Scan (PES) for proton transfer from RIF to IMQ.

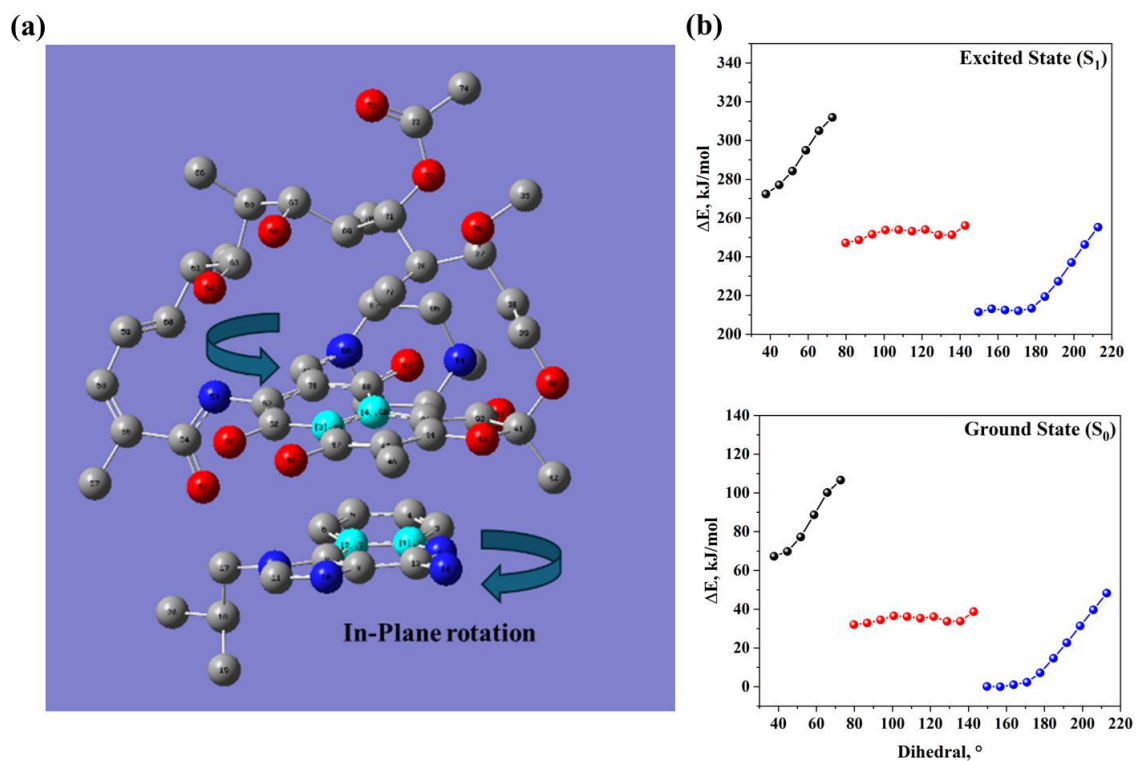


Fig. S13. Potential Energy Scan (PES) for dihedral angle during the in-plane rotation of IMQ with respect to RIF.